Interactions of N_2^+ and NO^+ Ions with Surfaces of Graphite, Diamond, Teflon, and Graphite Monofluoride

J. Ashley Taylor, Gerald M. Lancaster,† and J. Wayne Rabalais*

Contribution from the Department of Chemistry, University of Houston, Houston, Texas 77004. *Received January 11, 1978*

Abstract: Ion beam studies of the reactions of nitrogen and nitric oxide with surfaces of carbonaceous materials are reported. The techniques of x-ray and UV photoelectron spectroscopy (XPS and UPS) and thermal desorption mass spectrometry under ultrahigh vacuum conditions are used to examine the products induced by 30–500-eV N_2^+ and NO^+ beams on graphite, diamond, Teflon, and graphite monofluoride. The molecular ions undergo charge-exchange neutralization and dissociation at the surface to form hot N and O atoms. Reactions between these hot atoms and the surfaces produce a cyanide- and oxide-type bond with the carbon. In the case of graphite, two different reaction products are observed for reaction with either N or O atoms. It is proposed that one of these is the cyanide- or oxide-type compound and the other is interstitial N or O atoms between the layers of rings or at defect sites in the lattice. A model for this reaction is proposed which includes neutralization and dissociation of the ions followed by surface penetration and deceleration and finally reaction with the atoms of the lattice.

I. Introduction

Ion–molecule reactions in which the ion undergoes a single collision at a controlled energy with another reactant in a crossed beam provide data on the energy dependences of reaction cross sections and the product angular and velocity distributions. Detailed mechanistic inferences can be drawn from these data. If the molecule is replaced by a surface, i.e., ion–surface reactions, reactions of the ion with the infinite surface can be induced. Ions impingent on a surface can be reflected or they can penetrate the surface, losing energy in collision cascades with lattice atoms until they are eventually thermalized within the lattice. Once the ions are thermalized, their ultimate fate is determined by three processes: (1) diffusion to the surface and emission as gases, (2) physical entrapment in the lattice as neutral species, and (3) chemical reaction with the lattice atoms. The rate of process (1) is rapid for cases where there is little or no chemical affinity between the bombarding ion and target, e.g., He^+ and Ne^+ ions on Au. Process (2) involving physical implantation of neutral species surely occurs; however, considerably high ion doses are required in order to inject a sufficient quantity for detection.[1] The rate of process (3) can be rapid in cases where the chemical affinity between the impinging species and lattice atoms is high. We have recently shown[2,3] that in such cases, the rate of process (3) far surpasses that of process (2) and only low ion doses are required to produce easily detectable quantities of reaction products. The unique features of such "reactive ion bombardment" are the ability to alter the chemical nature of a surface and to induce highly specific and selective reactions through injection of specific mass and energy selected ions at precise spatial locations at known concentrations.

Experiments employing charge/mass and velocity selected ion beams as reactants are generally more manageable and flexible than those using molecular beams because of the simplicity of focusing and energy selecting ion beams. Several investigators[4–13] have shown that a fast ion approaching a surface undergoes charge exchange processes (resonance neutralization or Auger transitions) with the surface in which the ion becomes neutralized. The bombarding species are, therefore, essentially neutral atoms or molecules whose kinetic energies are virtually identical with those of the ions. By varying the kinetic energies of the ions from ~1 eV to thousands of eV, one can control their depth of penetration into the lattice and, hence, the thickness of the reacted layer. The impinging ions can react on initial or subsequent collisions or after becoming thermalized. Since there is little known about such energy-loss cross sections, it is difficult to convert reaction yields into reaction cross sections at present. However, through the use of surface-sensitive detection techniques and ultrahigh-vacuum technology, it is possible to analyze the reacted surface in situ and gain much fundamental information about the reaction processes involved.

Our recent work has shown that ion beams of N_2^+ can be used to induce *chemical reactions* between N atoms and group 4 elements and their oxides.[2,3] Bombardment of M, MO, and MO_2 (M = Si or Ge) with 500 eV N_2^+ results in the formation of nitrides which are similar to Si_3N_4 and Ge_3N_4. Reaction with tin and its oxides was barely detectable and no reaction was observed on Pb and its oxides in accord with the known instability of such nitrides. Variation of ion energy over the range 30–3000 eV produced no detectable changes in the chemical reaction; higher energies only served to drive the ions deeper into the target. The reaction of 500 eV N_2^+ with Si(100) forms a silicon nitride layer of ~19 Å thick as determined[3] by the film/bulk Si XPS intensity ratio and by depth-concentration profiling using 1 keV Ar^+.

This paper describes the reactions induced by 30–500 eV N_2^+ and NO^+ ions on polycrystalline and pyrolytic graphite and N_2^+ ions on diamond, graphite monofluoride, and Teflon. The techniques of x-ray and UV photoelectron spectroscopy (XPS and UPS) and mass spectrometric detection of thermally desorbed species under ultrahigh-vacuum conditions are used in analysis of reaction products. Emphasis is placed on the fact that *chemical reactions* occur in the solid as a result of reactive ion implantation. This is substantiated by studies of the energy level shifts in the bombarded materials, the effects of ion dose, and detection of thermally desorbed species.

II. Experimental Section

The experiments were performed in a bakeable ultrahigh-vacuum chamber designed for maximum flexibility and versatility in the use of x-ray and UV photoelectron spectroscopy (XPS and UPS), Auger electron spectroscopy (AES), secondary ion mass spectrometry (SIMS), and ion bombardment of surfaces. Base pressures down to the 10^{-11} Torr range are obtainable by means of a combination of a 450 L/s turbomolecular pump, a 500 L/s ion pump, and a titanium sublimation pump and cryopanel. The facility has been fully described elsewhere.[3] The instrumentation employed in this investigation consists of a Physical Electronics Industries, Inc. (PHI) double-pass cylindrical mirror electron analyzer, a PHI Al Kα x-ray source, a differentially pumped He I and He II source of our own design,[14] a Varian ion bombardment gun, and an Extranuclear Laboratories, Inc., SIMS. Two stages of differential pumping allow operation of the

† R. A. Welch Foundation Predoctoral Fellow.

0002-7863/78/1500-4441$01.00/0

Table I. Ionization Energies and Line Widths (in parentheses) in Electron Volts for Graphite, Diamond, Teflon, and CF before and after 500 eV Ion Bombardment[a]

	C 1s	N 1s	O 1s	F 1s
Graphite	284.6 (1.5)			
Graphite/N_2^+	284.6 (2.9)	398.5 (~2.0)		
		400.0 (~2.1)		
		[N 1s/C 1s = 0.18]		
Graphite/NO^+	284.6 (2.6)	398.9 (~2.0)	531.4 (2.2)	
		400.2 (~2.1)	533.1 (2.3)	
		[N 1s/C 1s = 0.12]	[O 1s/C 1s = 0.096]	
Diamond	285.0 (2.2)			
Diamond/N_2^+	285.0 (2.9)	398.5 (2.9)		
		[N 1s/C 1s = 0.072]		
Teflon	292.6 (2.0)			690.1 (2.3)
Teflon/N_2^+	287.6 (3.2)	401.6 (3.0)		689.6 (2.8)
	292.6 (2.6)			
CF	288.1 (2.3)			687.0 (2.3)
CF/N_2^+	285.8 (3.0)	399.4 (3.1)		687.1 (2.5)
	288.1 (2.7)			

[a] Ratios of the intensity of an XPS line of the bombarding ion to the intensity of the C 1s line of the target sample are indicated for graphite and diamond. The experimental XPS intensities were divided by the cross sections of the respective levels as obtained from J. H. Scoefield, *J. Electron Spectrosc.*, **8**, 129 (1976), in order to make the ratios independent of cross section.

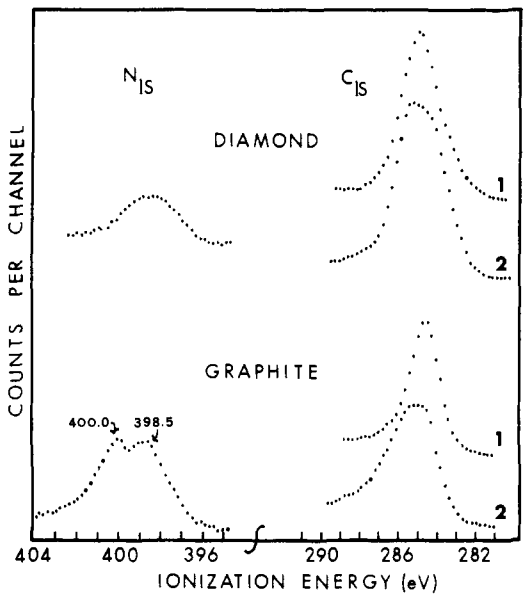

Figure 1. The C 1s and N 1s XPS spectra of diamond and pyrolytic graphite before (1) and after (2) N_2^+ bombardment.

windowless UV source while maintaining the pressure in the main sample chamber in the 10^{-10}-Torr range. XPS and UPS data were collected in a multichannel analyzer and then stored on a magnetic tape cassette for transfer to the University computer via a keyboard printer terminal and acoustical coupler.

Resolution (full width at half-maximum) in the XPS mode using Al Kα radiation is 1.2 eV (with a 15-eV pass energy) as measured on the Au $4f_{7/2}$ line. The UPS mode provides a resolution of 0.1 eV as determined from the $3p_{3/2}$ line of Ar vapor at 1×10^{-4} Torr. XPS spectra are calibrated to the Au $4f_{7/2}$ line at 84.0 eV. The UPS spectra are calibrated to the Fermi level of Au.

Ion bombardment experiments were performed by backfilling the chamber with the gas to be ionized to a pressure of $5\text{-}50 \times 10^{-6}$ Torr. Bombardment was performed under dynamic gas flow conditions with the turbomolecular pump open. This provides a continuous stream of fresh gas and serves to remove sputtered products from the chamber. The ion beams were rastered over the sample surface and ion currents were measured using a Faraday cup and a picoammeter. For insulating samples, a low-intensity electron beam impingent on the sample during ion bombardment assured neutralization. Mass spectrometric fragmentation patterns indicate that the nitrogen beam is composed of ~96% N_2^+ and ~4% N^+ and that the nitric oxide beam is composed of ~90% NO^+ and ~10% atomic ions such as N^+ and O^+.

Samples of pyrolytic and polycrystalline graphite in the form of thin disks were clamped onto the sample holder. The clamps serve as terminals for high-current leads that extend out of the vacuum chamber through UHV feedthroughs. Graphite temperatures ranging above 1000 °C were obtainable by placing a high current (up to 75 A) through the sample. Temperature was measured by means of a chromel-alumel thermocouple attached between the sample and clamp. Control of the temperature was obtained by an Omega Eng., Inc. proportioning controller. The graphite was cleaned by heating to 1200 °C for approximately 1 h. The gases evolved as a function of temperature from the bombarded graphite were detected by using the SIMS in the conventional mass spectrometric mode. Such measurements were made with the turbomolecular pump open in order that the evolved gases could be pumped continuously.

The sample of pyrolytic graphite was the x-ray monochromator grade obtained from the Union Carbide Co. Polycrystalline graphite disks were cut from a high-purity rod. A cleaved industrial diamond was mounted on a gold-coated stainless plate by using Torr Seal epoxy which was cured under vacuum at 150 °C. Thin Teflon sheets were obtained from Alpha Inorganics, Inc. Fluorinated graphite was prepared by heating polycrystalline graphite in the presence of fluorine gas. The resulting white powder had a composition of $CF_{1.14}$. Samples were prepared for bombardment by pressing the powder into 1-cm^2 disks.

III. Results

A. XPS Results. The ionization energies of graphite, diamond, Teflon, and CF before and after 500 eV ion bombardment are listed in Table I. Line widths (fwhm) are indicated in parentheses. Ionization energies of the pure samples are in good agreement with previous measurements on similar samples.[15,16] Ion bombarded samples are referred to as graphite/N_2^+, Teflon/N_2^+, etc. Most of the spectra were acquired with a cylindrical mirror analyzer pass energy of 50 eV, resulting in a fwhm of 1.7 eV for the Au $4f_{7/2}$ line. The ratios of the intensity of an XPS line of the bombarding ion to the intensity of the C 1s line of graphite and diamond are listed in Table I. These ratios represent the intensities obtained with the "saturation dose" of ions;[3] this is the minimum ion dose required to produce the maximum ion XPS signal in the sample. Intensity ratios were found to be strongly dependent on ion dose up to the saturation point and essentially independent of ion kinetic energy over the 30–3000-eV range. The saturation dose on graphite was approximately 7.2×10^{-3} A·s/cm^2.

Representative spectra of graphite and diamond showing

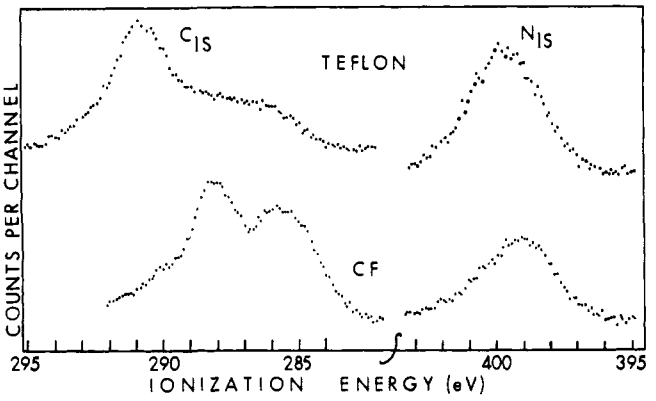

Figure 2. The C 1s and N 1s XPS spectra of Teflon and CF after N_2^+ bombardment. The C 1s spectra of Teflon and CF before bombardment consist of a single line at the position of the high binding energy component of this figure.

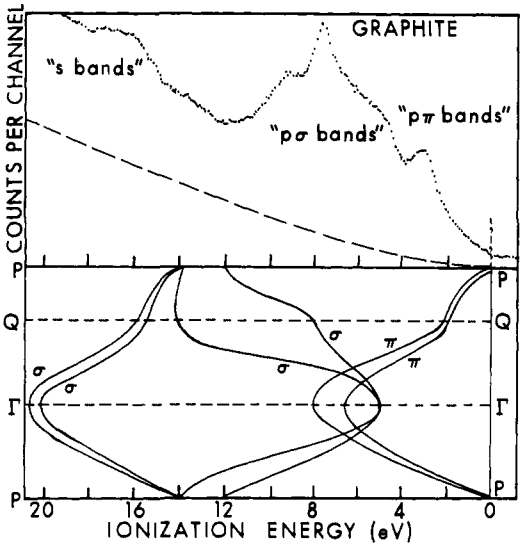

Figure 3. He II UPS spectrum of the valence bands of pyrolytic graphite along with the valence band structure of Willis et al. 0 = Fermi level.

the results of N_2^+ bombardment are shown in Figure 1. The C 1s lines of graphite/N_2^+ and diamond/N_2^+ are considerably broader (Table I) than those of the pure materials, indicating the presence of carbon in different chemical environments in the bombarded materials. The N 1s lines are very broad, particularly in graphite/N_2^+ where the peak consists of two overlapping components at 398.5 and 400 eV; only the low-energy component is present in diamond. Graphite/NO^+ spectra exhibit features similar to those of graphite/N_2^+, i.e., a broadened C 1s line and two N 1s and O 1s lines each. As listed in Table I, N_2^+ bombardment of graphite results in significant concentrations of nitrogen in the sample while N_2^+ bombardment of diamond yields a much lower concentration of nitrogen.

Representative spectra of the C 1s lines of Teflon and CF after N_2^+ bombardment are shown in Figure 2. In both targets the single C 1s line of the pure samples is split into two distinct components in the bombarded samples, i.e., a new broad C 1s line is observed at lower binding energy. This lower energy component comprises ~27% of the total C 1s intensity in Teflon/N_2^+ and ~43% in CF/N_2^+. The N 1s line of Teflon/N_2^+ and CF/N_2^+ is very broad and located near the position of the high-energy N 1s line of graphite/N_2^+ and graphite/NO^+.

B. UPS Results. The He II UPS spectrum of pyrolytic graphite along with the graphite valence band structure of Willis et al.[17] obtained from ab initio band structure calculations is shown in Figure 3. The He I UPS spectrum of graphite[18,19] and the XPS spectrum of pyrolytic graphite[15] have been reported; however, this appears to be the first He II spectrum of pyrolytic graphite. Our spectrum is in good agreement with those reported previously; differences in relative band intensities occur because of the variation of C 2s and 2p cross sections as a function of incident photon energy and the different excitation and collection angles used in different experimental apparatus. The discernible fine structure observed in the He II spectrum deserves comparison with the band structure calculation.[17]

Graphite consists of layers of fused hexagonal rings with four atoms in the primitive unit cell. The layered structure causes a grouping of the bands into two π bands formed from the 2p(π) type functions and six σ bands formed from the 2s and 2p(σ) type functions. A qualitative understanding of the graphite valence bands can be obtained by comparison of the spectrum with the band structure calculation of Willis et al.[17] The lowest energy band extending from the Fermi level to ~4 eV and peaking at 3 eV is due to the pure pπ bands formed from the p functions that are perpendicular to the layers of rings. The calculation indicates that these bands become flat near the Q point in the Brillouin zone, producing a high density of states. The next feature consists of a shoulder at ~5 eV corresponding to the top of the σ bands which are flat near the Γ point. The sharp peak at 7.6 eV and the broad structure at 9 eV arise from the flat region of the pπ bands near the Γ point. In this energy region the σ bands also exhibit some shallow-sloping regions near Q and contribute to the density of states. The weak structure near 13.7 eV corresponds to the flat σ bands near the P point. The bottom of the valence band is composed entirely of σ type functions, with the lower density of states due to the flat σ bands near the Γ point at ~20 eV. Agreement between the experimental density of states and the theoretical band structure calculation is qualitatively very good.

The UPS spectra of polycrystalline graphite, pyrolytic graphite/N_2^+, and polycrystalline graphite/NO^+ are shown in Figure 4. The spectrum of polycrystalline graphite/N_2^+ is identical with that of pyrolytic graphite/N_2^+. The spectrum of polycrystalline graphite exhibits the basic features of the spectrum of Figure 3; however, the structure is significantly broadened. Bombardment by N_2^+ and NO^+ produces shifts in the peaks and, in some cases, new structures. There is a noticeable recession of the density of pπ states near the Fermi level in the N_2^+ and NO^+ bombarded graphite. The bombarding ions obviously perturb the density of states of graphite substantially; furthermore, different ions appear to provide a different perturbation on the band structure.

C. Thermal Decomposition of Bombarded Graphite. Thermal decomposition curves for pyrolytic graphite bombarded with N_2^+ showing evolved N and CN are presented in Figure 5. The N and CN were detected by using the SIMS in the conventional residual gas analyzer mode in which gaseous species are ionized by electron bombardment to form positive ions. It is difficult to observe molecular nitrogen because of the CO which is produced from the reaction of hot graphite with the residual oxygen in the chamber. However, we did observe that the total amount of mass 28 evolved upon heating graphite and bombarded graphite remained constant. This indicates that N_2 evolution is minimal. Evolution of atomic nitrogen begins at ~140 °C and proceeds at a low rate up to about 700 °C; at this point evolution is rapid, peaking at ~1000 °C. This suggests that there are probably two different types of nitrogen in the sample which are evolved at different temperatures. Evolution of CN follows the N from ~140 °C to ~800 °C; above 800 °C the CN signal decreases smoothly. The presence

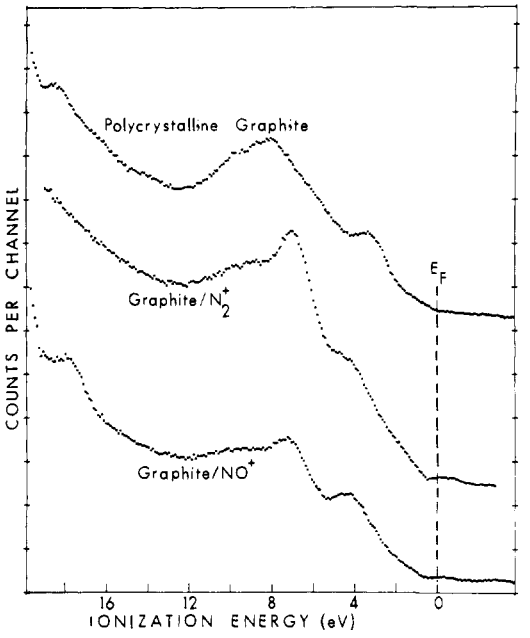

Figure 4. He II UPS spectra of polycrystalline graphite, pyrolytic graphite/N_2, and polycrystalline graphite/NO^+.

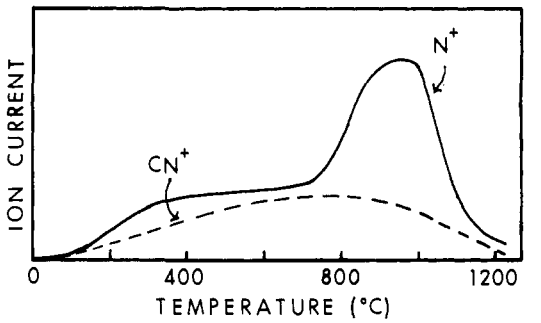

Figure 5. Thermal decomposition curves for pyrolytic graphite bombarded with 500 eV N_2^+ showing evolved N and CN. The evolved species were detected by mass spectrometry using electron bombardment ionization.

of a CN signal indicates that the nitrogen is reacting with the graphite; however, it is not possible to determine to what extent this reaction is induced by the high temperature. After heating the sample to ~1200 °C and expelling all of the N and CN, the sample can be cooled and reheated with no observable emission of either species.

IV. Discussion

The data presented in the previous section indicate that bombardment of graphite by N_2^+ and NO^+ and bombardment of diamond, Teflon, and CF by N_2^+ results in chemical reactions between the target and the impinging species. The observations that suggest such reactions can be summarized as follows: (1) Two N 1s peaks are present in graphite/N_2^+. (2) Two N 1s and two O 1s peaks are present in graphite/NO^+. (3) Only one N 1s peak is present in diamond/N_2^+. (4) Nitrogen evolution occurs at two different rates as a function of temperature and CN is evolved commensurate with the nitrogen when graphite/N_2^+ is heated. (5) An additional "reduced" carbon 1s peak is present in Teflon/N_2^+ and CF/N_2^+. (6) The valence bands of graphite are perturbed differently by N_2^+ or NO^+ bombardment. (7) Large variations occur in the saturation concentration of reactant in the target samples.

A. Product Identification. The broadening of the C 1s line of graphite/N_2^+ and diamond/N_2^+ is due to chemical shifts from bonding with the nitrogen. The N 1s line at 398.5 eV is similar to the binding energies of partially negative cyanide-type nitrogens. The additional N 1s peak at 400.0 eV in graphite/N_2^+, which is absent in diamond, is similar to the binding energies of more neutral nitrogen species. Graphite is known to react with a large number of substances to form three different types of interstitial compounds.[20] *Nonconducting compounds* of graphite have extensively altered structures from that of pure graphite, the metallic properties are completely lacking and the carbon layers are no longer planar as a result of strong bonding of carbon to other species. *Lamellar compounds* retain the aromatic, planar graphite layer structure and semimetallic properties, while intercalating uniform monolayers of reactant between the carbon layers. *Residue compounds* retain the reactant at imperfections and peripheral surfaces of the graphite crystallites, their properties varying considerably as a function of the nature and concentration of the reactant. The cyanide-like N 1s XPS peak (398.5 eV), the high temperature (~1000 °C) necessary to decompose the product, and the evolution of CN indicate that a nonconducting cyanide-type compound of graphite, graphite nitride, is being formed which is of the graphite oxide or graphite monofluoride type. In such a graphite nitride, the more electronegative nitrogen will withdraw electron density from the carbon, hence producing a partially negative nitrogen species. The corresponding compound can be formed in diamond if the kinetic energy of the impinging N_2^+ breaks some of the C–C bonds, allowing the formation of a similar cyanide species.

The nitrogen 1s peak at 400.0 eV and the evolution of nitrogen from ~140 to ~700 °C indicate that some of the nitrogen is held in a more neutral, less tightly bound state. Such a species could be either a residue or lamellar compound. The former is probably the best description, for it is unlikely that N_2^+ bombardment will produce uniform well-defined layers of reactant between the layers of graphite rings. It is more probable that the nitrogen will be trapped as neutral species at lattice imperfections and twinning planes.

In compounds of graphite it is found that the conductivity is decreased or increased according to whether the intersitual species is highly electronegative or electropositive, respectively. The UPS spectrum of graphite/N_2^+ shows a decreased density of states near the Fermi level, indicating that the conductivity of the reacted layer should be altered. The density of states near the Fermi level is due to C $2p\pi$ electrons in orbitals perpendicular to the graphite layers. Introduction of the more electronegative nitrogen stabilizes these C 2p electrons and draws them from the Fermi level as a result of the formation of partially positive cyanide-like carbon.

The results for graphite/NO^+ indicate that nitrogen–carbon species similar to the ones discussed above are formed along with two different types of oxygen species. These two oxygen species are believed to correspond to nonconducting and residual graphite compounds with oxygen which are similar to the nitrogen compounds. Neither the nitrogen nor the oxygen XPS signals appear to correspond to an NO-like species. Reasons for this are discussed in the next section.

In Teflon/N_2^+ and CF/N_2^+, the appearance of a lower binding energy C 1s XPS peak in addition to the XPS peak of the pure material can be attributed to the reduction of C by fluorine evolution and the replacement of fluorine atoms by less electronegative nitrogen atoms. A more negative or lower binding energy C 1s XPS peak is expected in a replacement of the type $-CF_2-$ to $-NCF-$ in Teflon or CF to $CF_{1-x}N_x$ in fluorinated graphite. The position of the N 1s XPS line is higher than those of pure cyanide types owing to the highly electronegative fluorine atoms in the environment and, in some cases, attached to the same carbon atom. The nitrogen does not form NF species within the lattice, for such species contain a partially positive nitrogen whose N 1s XPS energy is in the range ~403–407 eV. The weak N 1s XPS signal in Teflon and

CF as compared to graphite indicates that only a small amount of nitrogen is reacting with the carbon. Thus, the low-energy C 1s XPS peak is evidently due to (1) reduction of carbon with subsequent nitrogen and fluorine evolution and (2) replacement of the more electronegative fluorine by nitrogen.

B. Nature of the Reacting Species. We are concerned here with identifying the nature of the reacting species. It has been shown that energetic ions approaching a surface have a high probability of becoming neutralized and reacting as hot atoms or molecules. Experiments by Wolfgang et al.,[4-6] Lemmon et al.[7-9] Cooks et al.,[21] and Winters et al.[13] using a variety of ions and targets have demonstrated that efficient charge transfer occurs near the surface. Hagstrum[11,12] has studied the mechanisms for neutralization of ions on metal and semiconductor surfaces. He has found that charge exchange between the ion and surface in the form of *resonance neutralization* or *Auger neutralization* is efficient and rapid at distances of ~5–6 Å from the surface. We employ these basic ideas in the following discussion.

Energetic N_2^+ ions approaching a surface can undergo *resonance neutralization*[12] in which an electron from the surface tunnels through the potential barrier between the solid and ion to populate a resonant level in the ion. Such a process is illustrated by the dashed line in Figure 6 for the case of a grounded graphite surface and approaching N_2^+ and N^+ ions. The valence band of graphite extends from 4.6 to ~22 eV below the vacuum level. The molecular energy levels of N_2 in this energy range are $3\sigma_g$ (15.5 eV), $1\pi_u$ (16.7 eV), and $2\sigma_u$ (18.8 eV). Approaching N_2^+ ions of the configuration—$2\sigma_u^2\, 1\pi_u^4\, 3\sigma_g^1$, $^2\Sigma_g$ can be resonance neutralized by 15.5 eV electrons in the graphite valence band. This process is also expected for N_2^+ in the $^2\Pi_u$ and $^2\Sigma_u$ excited states, for both the $1\pi_u$ and $2\sigma_u$ levels have resonant counterparts in graphite. Approaching ground-state ^2P N^+ ions have a vacancy in the 2p shell at 14.5 eV and can undergo these same processes. Approaching NO^+ and O^+ ions also have vacant levels in this range available for resonance neutralization. Insulators such as Teflon and CF have broad valence bands extending down to ~30 eV below the vacuum level and, hence, can undergo the same processes.

The valence band in metals is usually narrow and extends to only ~12 eV (depending upon the width of the valence band) below the vacuum level. Neither N_2^+ nor N^+ has levels available in this range for resonance change transfer. In such cases, *Auger neutralization*[12] takes place between the metal and ion. This process involves tunneling of a metal valence band electron through the potential barrier to occupy a lower level in the ion as illustrated by the solid arrows in Figure 6; the energy gained in the process excites another metal electron into the conduction band or vacuum, depending upon its excitation energy.

Studies[4] over the energy range 1–1000 eV have shown that cross sections for such charge exchange processes are large (~100 Å^2) and essentially independent of kinetic energy. Cross sections for ion–molecule reactions are considerably smaller than those for charge-transfer above about 5 eV. From these considerations we conclude that *N_2^+ and NO^+ ions are neutralized before striking the surface (~5–6 Å from the surface) and continue as neutral species with the same kinetic energy.* Interaction potentials at these distances are small and the electron transfers negligible momentum; therefore, the initial kinetic energy remains unchanged. The minima in the potential energy curves for the ground state of the molecular ion and the ground state of the molecule occur at approximately the same internuclear distance. Hence, application of the Franck–Condon principle to the neutralization reaction suggests that the molecule is formed in its ground electronic state without significant vibrational excitation.[13]

Our own experimental results also provide evidence for neutral reactants. If N_2^+ or N^+ ions would be reacting, we would expect to form products such as NF in which the nitrogen accepts a partial positive charge; no evidence for positive nitrogen species was found in the XPS spectra of bombarded Teflon and CF.

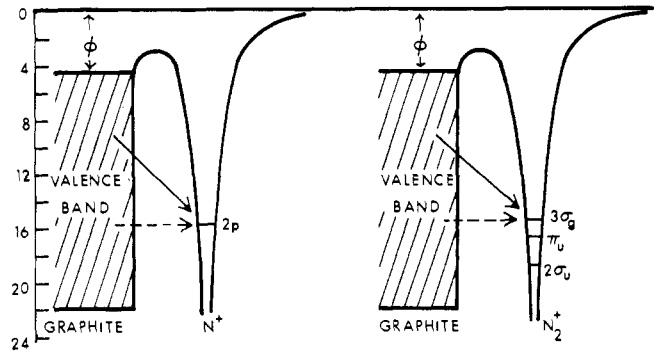

Figure 6. Schematic diagram illustrating resonance neutralization (dashed arrow) and Auger neutralization (solid arrows) of an ion near a surface. ϕ represents the work function of graphite.

The N_2 and NO molecules at 500 eV formed by neutralization of the ions have a high probability of undergoing collision-induced dissociation at the surface to yield N and O atoms. The kinetic energy which remains after collision and dissociation is distributed to the pair of atoms in proportions which are determined by the orientation of the molecule upon collision. The energy required for such a collisional dissociation has been shown[13] to be ~9 eV, i.e., near the dissociation energy of the free molecule. Therefore, the two resulting atoms will have average energies of nearly 250 eV each. We believe that *a large percentage of the N_2 and NO at the surface ends up as N and O atoms* for the following reasons. It is highly unlikely that the reacting species is the molecule because of the stability and low reactivity of N_2. When our vacuum chamber is backfilled with N_2 or NO, we observe no nitrogen or oxygen in the samples within our detectability limits. If NO would be reacting as a molecule, we would expect to observe a partially positive N 1s XPS peak in graphite/NO^+; this was not observed. Also it will be shown in a later section that we have an insufficient number of N^+ and O^+ ions in the beams to attribute the entire reaction to neutralized atomic ions. The N_2^+ and NO^+ must be reacting in order to obtain a sufficient number of N atoms. The atoms formed on the surface with ~250 eV penetrate the lattice, losing energy in collision cascades until they are slowed down sufficiently to react with atoms of the bulk.

C. Ion Penetration and Concentration. The projected range of the bombarding ions in the target can be calculated from LSS theory.[22] Assuming that N_2^+ dissociates at the surface to form two N atoms, each with 250 eV kinetic energy, their range in graphite will be ~14 Å. Treating the impinging 500 eV N_2^+ as nonreactive billiard balls of mass 28, their projected range will be ~17 Å. If all the 500 eV is imparted to one N atom, its range will be ~23 Å. Our saturation dose of 7.2×10^{-3} A·s/cm^2 for nitrogen on graphite corresponds to $\sim 4.5 \times 10^{16}$ ions/cm^2 of composition ~96% N_2^+ and ~4% N^+. At 500 eV essentially all N_2^+ ions dissociate upon collision yielding a total of 8.82×10^{16} N atoms available for reaction. Using the interplanar spacing of graphite (3.35 Å) and an average projected N atom range of ~16 Å, the nitrogen is dispersed among ~five graphite planes. In terms of monolayers, this indicates ~four to five monolayers of nitrogen. A monolayer of nitrogen atoms consists of $\sim 3 \times 10^{15}$ atoms/cm^2. Hence, if five monolayers are formed, then approximately 17% of the N atoms are reacting with the graphite and remaining in the lattice. The percent of original ions (N_2^+ and N^+) reacting is ~33%. It should be noted that the amount of original N^+ ions in the beam, 1.8×10^{15} ions/cm^2, is not sufficient to provide

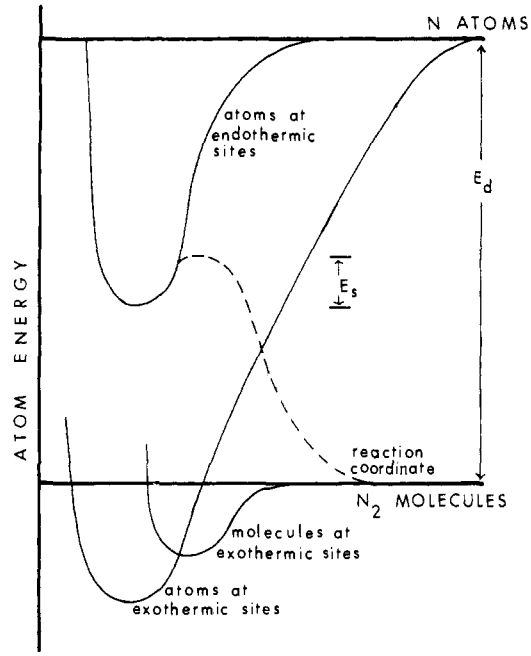

Figure 7. Schematic potential energy diagram for nitrogen reacting with graphite. E_d represents the dissociation of N_2 and E_s denotes the activation energy for surface diffusion. The solid curves indicate energies in a direction perpendicular to the surface while the dashed curve shows potential energy in the plane of the surface. This dashed curve represents diffusion of surface N atoms to form N_2.

even a single monolayer of nitrogen. This is further evidence for dissociation of the nitrogen molecules at the surface.

D. Reaction Model. The energy of an ion approaching a surface is composed of three parts, i.e., the internal excitation energy of the ion, the interaction energy between the surface and the ion, and the kinetic energy of the ion. The first contribution, excitation energy of the ion, is represented by its ionization potential. The ion is neutralized into the electronic ground state of the molecule while it is still several ångstroms from the surface. Dissociation of ground-state N_2 at the surface most likely produces ground-state N atoms according to the adiabatic principle and similar physical principles relating to interchange of kinetic and internal energy. The second contribution, interaction between the surface and ion, can to a first approximation be considered as an image potential, $I = -e^2/4s$, where s is the surface–ion distance. Since the ion is neutralized several ångstroms from the surface, this potential is small. The attractive interaction between the neutral N_2 and the graphite surface is also small since adsorption or reaction does not occur at ambient conditions. The third contribution, the kinetic energy of the ion, should therefore be the primary source of activation energy for reaction. This is substantiated by the ~9 eV kinetic energy threshold[13] that has been observed for the reaction. Kinetic energies in excess of ~9 eV are dissipated in collision cascades.

The energetics of the processes which occur when a clean graphite surface is exposed to nitrogen can be represented qualitatively by the potential energy diagram of Figure 7. Potential energy curves for the reaction of nitrogen molecules and atoms with graphite are indicated. The curves representing N_2 and N at exothermic sites correspond to cases where the energy change in going from the molecular gas to the reacted molecules or atoms is negative. Such reactions should occur at ambient conditions; since they do not occur, these potential wells must not exist. In the endothermic reaction, the energy change in going from the molecular gas to the reacted atoms is positive. Hence, the energy of the reacted atom is greater than its energy would be as part of a gas-phase molecule. This explains why exposure to the molecular gas does not populate these sites. Although the site is endothermic, the atom can still be strongly bound to the graphite since it would require energy to release it as a gaseous atom. Release as a gaseous molecule requires that the atoms acquire the activation energy for surface diffusion in order to move along the potential curve indicated by the dashed line. The two N 1s XPS peaks and the evolution of N at different temperatures suggest that there are really two endothermic atomic reaction sites.

The elementary steps in this complex reaction mechanism, using a graphite surface, can be expressed as follows, where the subscripts g, s, and b denote gaseous, surface, and bulk species, respectively, and G denotes graphite.

$N_2^+(500\text{ eV})_g + e_G^- \rightarrow N_2(500\text{ eV})_g$	charge exchange	(1)
$N^+(500\text{ eV})_g + e_G^- \rightarrow N(500\text{ eV})_g$		(2)
$N_2(500\text{ eV})_g + G_s \rightarrow 2N(\sim 250\text{ eV})_s$	dissociation at surface	(3)
$N(500\text{ eV})_g + G \rightarrow N_b$	penetration of atoms	(4)
$2N(250\text{ eV})_s + G \rightarrow 2N_b$	into bulk	(5)
$N + G \rightarrow -\overset{\vert}{\underset{\vert}{C}}N$	chemical reaction	(6)

Reactions 1 and 2 describe charge exchange with the graphite surface and reaction 3 represents dissociation at the surface. Penetration of the atoms into the bulk is depicted in reactions 4 and 5 and final chemical reaction of the near thermalized nitrogen is denoted in reaction 6.

V. Conclusions

We have shown that ion beams of N_2^+ and NO^+ can be used to induce chemical reactions of N and O atoms with surfaces of graphite, diamond, Teflon, and graphite monofluoride. The identification of the products through XPS chemical shifts, changes in valence band density of states, and thermal desorption of N and CN species vindicate that the interaction is of a chemical nature. Reaction of N and O with graphite produces two products, a cyanide or oxide type of compound and interstitial N or O atoms between the layers of rings or at defect sites. Reaction of N with the other carbonaceous materials produces only a cyanide-type compound. Ion kinetic energy in the range 30–3000 eV appears to be insignificant in the reaction; it only serves to drive the ions deeper into the target.

The selectivity and specificity of these beam-surface reactions, as demonstrated here, suggest the use of such techniques for preparing surfaces with unique properties. The advantage of this "reactive ion implantation" is the ability to *alter the chemical nature of a surface.*

Acknowledgment is made to the donors of the Petroleum Research Fund, administered by the American Chemical Society, and to the U.S. Army Office of Research for support of this research.

References and Notes

(1) P. H. Citrin and D. R. Hamann, *Chem. Phys. Lett.*, **22**, 301 (1973).
(2) J. A. Taylor, G. M. Lancaster, and J. W. Rabalais, *J. Electron Spectrosc. Relat. Phenom.*, in press.
(3) J. A. Taylor, G. M. Lancaster, A. Ignatiev, and J. W. Rabalais, *J. Chem. Phys.*, **68**, 1776 (1978).
(4) M. Menzinger and R. Wolfgang, *J. Chem. Phys.*, **50**, 2991 (1969).
(5) R. L. LeRoy, A. J. Yencha, M. Menzinger, and R. Wolfgang, *J. Chem. Phys.*, **58**, 1741 (1973).
(6) S. Durana, R. L. LeRoy, M. Menzinger, and A. J. Yencha, *J. Chem. Phys.*, **60**, 2568 (1974).
(7) R. M. Lemmon, *Acc. Chem. Res.*, **6**, 65 (1973).
(8) H. M. Pohlit, W. R. Erwin, F. L. Reynolds, R. M. Lemmon, and M. Calvin, *Rev. Sci. Instrum.*, **41**, 1012 (1970).

(9) H. M. Pohlit, T. H. Lin, W. R. Erwin, and R. M. Lemmon, *J. Am. Chem. Soc.*, **91**, 5421 (1969); *J. Phys. Chem.*, **75**, 2555 (1971).
(10) G. M. Jenkins and D. R. Wiles, *J. Chem. Soc., Chem. Commun.*, 1177 (1972).
(11) H. D. Hagstrum, *Phys. Rev.*, **96**, 336 (1954); **150**, 495 (1966); **119**, 940 (1960); *Surf. Sci.*, **54**, 197 (1976); *Metals*, **6**, 309 (1972).
(12) H. D. Hagstrum, *Phys. Rev.*, **122**, 83 (1961).
(13) H. F. Winters and D. E. Horne, *Surf. Sci.*, **24**, 587 (1971); H. F. Winters, *J. Appl. Phys.*, **43**, 4809 (1972); H. F. Winters and P. Sigmund, *ibid.*, **45**, 4760 (1974).
(14) G. M. Lancaster, J. A. Taylor, A. Ignatiev, and J. W. Rabalais, *J. Electron Spectrosc. Relat. Phenom.*, in press.
(15) F. R. McFeely, S. P. Kowalezyk, L. Ley, R. G. Cavel, R. A. Pollak, and D. A. Shirley, *Phys. Rev.*, **9**, 5268 (1974).
(16) C. R. Ginnard and W. M. Riggs, *Anal. Chem.*, **44**, 1310 (1972).
(17) R. F. Willis, B. Fitton, and G. S. Painter, *Phys. Rev. Sect. B*, **9**, 1926 (1974).
(18) P. M. Williams, D. Latham, and J. Wood, *J. Electron Spectrosc. Relat. Phenom*, **7**, 281 (1975).
(19) A. M. Bradshaw and U. Krause, *Verlag Chem.*, 1095 (1975).
(20) G. Henning, *J. Chem. Phys.*, **19**, 922 (1951); M. L. Dzurus and G. R. Henning, *J. Am. Chem. Soc.*, **9**, 1051 (1957); G. Henning, *J. Chem. Phys.*, **20**, 1438 (1952); H. Selig, P. K. Gallagher, and L. B. Ebert, *Inorg. Nucl. Chem. Lett.*, **13**, 427 (1977); M. E. Vol'pin, Yu. N. Nivokov, N. D. Lapkina, V. I. Kasatochkin, Yu. T. Struckhov, M. E. Kazahov, R. A. Stukan, V. A. Povitskij, Yu. S. Karimov, and A. V. Zuarikina, *J. Am. Chem. Soc.*, **97**, 3366 (1975).
(21) V. Franchetti, B. H. Solka, W. E. Baitinger, J. W. Amy, and R. G. Cooks, *Int. J. Mass. Spectrom. Ion Phys.*, **23**, 29 (1977).
(22) The projected range is defined as the mean penetration depth for ions traveling normal to the surface; see P. D. Townsend, J. C. Kelly, and M. E. W. Hartley, "Ion Implantation, Sputtering, and Their Applications", Academic Press, New York, N.Y., 1976.

Preparation and Properties of Dinitrogen–Molybdenum Complexes. 6.[1] Syntheses and Molecular Structures of a Five-Coordinate Mo(0) Complex $Mo(CO)(Ph_2PCH_2CH_2PPh_2)_2$ and a Related Six-Coordinate Complex $Mo(CO)(N_2)(Ph_2PCH_2CH_2PPh_2)_2 \cdot {}^1/_2C_6H_6$

Maki Sato,[2a] Takashi Tatsumi,[2a] Teruyuki Kodama,[2a] Masanobu Hidai,*[2a] Tokiko Uchida,[2b] and Yasuzo Uchida[2a]

Contribution from the Department of Industrial Chemistry, Faculty of Engineering, University of Tokyo, Hongo, Tokyo 113, Japan, and Department of Industrial Chemistry, Faculty of Science and Technology, Science University of Tokyo, Noda, Chiba 278, Japan.
Received January 24, 1977

Abstract: The reaction of *trans*-$Mo(N_2)_2(dpe)_2$ (dpe = $Ph_2PCH_2CH_2PPh_2$) with benzyl propionate at reflux in benzene under dinitrogen yielded *trans*-$Mo(CO)(N_2)(dpe)_2 \cdot {}^1/_2C_6H_6$. On bubbling argon gas into a solution of the latter complex, a stable five-coordinate complex $Mo(CO)(dpe)_2$ was obtained and this reaction was reversible. The structures of those two complexes have been determined from three-dimensional x-ray counter data. The complex $Mo(CO)(dpe)_2$ crystallizes in the monoclinic system with the space group $P2_1/n$, with the following cell dimensions: a = 17.849 (3), b = 24.295 (4), c = 10.939 (2) Å; β = 99.117 (4)°, V = 4683.5 (13) Å^3, and Z = 4. The molybdenum atom has square-pyramidal coordination with four phosphorus atoms as a basal plane and an axial linear carbonyl ligand (average Mo–P = 2.452 (2) Å, Mo–C = 1.903 (9) Å, and C–O = 1.192 (12) Å). The nearest hydrogen is 2.98 (11) Å from molybdenum, suggesting van der Waals contact of the ortho hydrogen atom of one of the dpe phenyl groups with the metal. The complex $Mo(CO)(N_2)(dpe)_2 \cdot {}^1/_2C_6H_6$ crystallizes in the monoclinic system with the space group $C2/c$, with the following cell dimensions: a = 48.50 (6), b = 11.07 (1), c = 18.25 (2) Å; β = 97.98 (3)°, V = 9699 (22) Å^3, and Z = 8. The molybdenum atom has octahedral coordination with average Mo–P = 2.448 (4) Å, Mo–C = 1.973 (16) Å, Mo–N = 2.068 (12) Å, C–O = 1.127 (20) Å, and N–N = 1.087 (18) Å. Bond distances in two complexes are compared and discussed.

In a previous communication,[3] we briefly reported that a stable five-coordinate Mo(0) complex, $Mo(CO)(dpe)_2$ (dpe = $Ph_2PCH_2CH_2PPh_2$) (**1**), was obtained on bubbling argon gas into a benzene solution of *trans*-$Mo(CO)(N_2)(dpe)_2 \cdot {}^1/_2C_6H_6$ (**2**) and this reaction was reversible. Since structural information on metal sites which have the capacity to bind dinitrogen as a ligand is strongly desirable, it seems of special interest to determine the molecular structure of **1**. Furthermore, the five-coordinate M(0) complexes (M = Cr, Mo, or W) are frequently postulated as the intermediates in S_N1 processes of six-coordinate group 6 metal complexes[4] and the structures of such species have been extensively studied by trapping them in low-temperature solid matrices.[5] Although a few examples of five-coordinate d^6 complexes of Ru(II) and Rh(III) have been established by x-ray diffraction studies,[6] none is, to the best of our knowledge, known for group 6 transition metal complexes.[7] We wish here to report the synthesis and the molecular structure of the first example of a stable five-coordinate d^6 molybdenum complex **1**, as well as of the dinitrogen complex **2**.

Experimental Section

All reactions were carried out under an atmosphere of pure dinitrogen or argon using purified dioxygen-free solvents and standard Schlenk-tube techniques. The complex *trans*-$Mo(N_2)_2(dpe)_2$ was prepared by the published method.[8] Infrared spectra were recorded from KBr pellets using a Nihon-bunko IRAl double-beam spectrometer.

Preparation of *trans*-$Mo(CO)(N_2)(dpe)_2 \cdot {}^1/_2C_6H_6$ (2). Method A. Dimethylformamide (DMF) (19.0 g, 0.26 mol) was added to a solution of *trans*-$Mo(N_2)_2(dpe)_2$ (2.0 g, 2.1 mmol) in benzene (80 mL) under dinitrogen. The mixture was heated under reflux for 20 min, during which the orange solution had become dark red. After cooling, *n*-hexane (100 mL) was added and the precipitate formed was filtered off, washed with ether and *n*-hexane, and dried in vacuo to yield dark

0002-7863/78/1500-4447$01.00/0